

Observation of $h_b(1P) \rightarrow \eta_b(1S)\gamma$

- I. Adachi,¹³ K. Adamczyk,⁴⁴ H. Aihara,⁶⁷ K. Arinstein,² Y. Arita,³⁸ D. M. Asner,⁵⁰
 T. Aso,⁷¹ V. Aulchenko,² T. Aushev,²⁴ T. Aziz,⁶² A. M. Bakich,⁶¹ Y. Ban,⁵² E. Barberio,³⁷
 A. Bay,³² I. Bedny,² M. Belhorn,⁵ K. Belous,²¹ V. Bhardwaj,⁵¹ B. Bhuyan,¹⁶
 M. Bischofberger,⁴⁰ S. Blyth,⁴² A. Bondar,² G. Bonvicini,⁷³ A. Bozek,⁴⁴ M. Bračko,^{35, 25}
 J. Brodzicka,⁴⁴ O. Brovchenko,²⁷ T. E. Browder,¹² M.-C. Chang,⁶ P. Chang,⁴³ Y. Chao,⁴³
 A. Chen,⁴¹ K.-F. Chen,⁴³ P. Chen,⁴³ B. G. Cheon,¹¹ K. Chilikin,²⁴ R. Chistov,²⁴
 I.-S. Cho,⁷⁵ K. Cho,²⁸ K.-S. Choi,⁷⁵ S.-K. Choi,¹⁰ Y. Choi,⁶⁰ J. Crnkovic,¹⁵ J. Dalseno,^{36, 63}
 M. Danilov,²⁴ A. Das,⁶² Z. Doležal,³ Z. Drásal,³ A. Drutskoy,²⁴ Y.-T. Duh,⁴³
 W. Dungel,²⁰ D. Dutta,¹⁶ S. Eidelman,² D. Epifanov,² S. Esen,⁵ J. E. Fast,⁵⁰ M. Feindt,²⁷
 M. Fujikawa,⁴⁰ V. Gaur,⁶² N. Gabyshev,² A. Garmash,² Y. M. Goh,¹¹ B. Golob,^{33, 25}
 M. Grosse Perdekamp,^{15, 55} H. Guo,⁵⁷ H. Ha,²⁹ J. Haba,¹³ Y. L. Han,¹⁹ K. Hara,³⁸
 T. Hara,¹³ Y. Hasegawa,⁵⁹ K. Hayasaka,³⁸ H. Hayashii,⁴⁰ D. Heffernan,⁴⁹ T. Higuchi,¹³
 C.-T. Hoi,⁴³ Y. Horii,⁶⁶ Y. Hoshi,⁶⁵ K. Hoshina,⁷⁰ W.-S. Hou,⁴³ Y. B. Hsiung,⁴³
 C.-L. Hsu,⁴³ H. J. Hyun,³¹ Y. Igarashi,¹³ T. Iijima,³⁸ M. Imamura,³⁸ K. Inami,³⁸
 A. Ishikawa,⁵⁶ R. Itoh,¹³ M. Iwabuchi,⁷⁵ M. Iwasaki,⁶⁷ Y. Iwasaki,¹³ T. Iwashita,⁴⁰
 S. Iwata,⁶⁹ I. Jaegle,¹² M. Jones,¹² T. Julius,³⁷ H. Kakuno,⁶⁷ J. H. Kang,⁷⁵ P. Kapusta,⁴⁴
 S. U. Kataoka,³⁹ N. Katayama,¹³ H. Kawai,⁴ T. Kawasaki,⁴⁶ H. Kichimi,¹³ C. Kiesling,³⁶
 H. J. Kim,³¹ H. O. Kim,³¹ J. B. Kim,²⁹ J. H. Kim,²⁸ K. T. Kim,²⁹ M. J. Kim,³¹
 S. H. Kim,¹¹ S. H. Kim,²⁹ S. K. Kim,⁵⁸ T. Y. Kim,¹¹ Y. J. Kim,²⁸ K. Kinoshita,⁵
 B. R. Ko,²⁹ N. Kobayashi,^{54, 68} S. Koblitz,³⁶ P. Kodyš,³ Y. Koga,³⁸ S. Korpar,^{35, 25}
 R. T. Kouzes,⁵⁰ M. Kreps,²⁷ P. Križan,^{33, 25} T. Kuhr,²⁷ R. Kumar,⁵¹ T. Kumita,⁶⁹
 E. Kurihara,⁴ Y. Kuroki,⁴⁹ A. Kuzmin,² P. Kvasnička,³ Y.-J. Kwon,⁷⁵ S.-H. Kyeong,⁷⁵
 J. S. Lange,⁷ I. S. Lee,¹¹ M. J. Lee,⁵⁸ S.-H. Lee,²⁹ M. Leitgab,^{15, 55} R. Leitner,³ J. Li,⁵⁸
 X. Li,⁵⁸ Y. Li,⁷² J. Libby,¹⁷ C.-L. Lim,⁷⁵ A. Limosani,³⁷ C. Liu,⁵⁷ Y. Liu,⁴³ Z. Q. Liu,¹⁹
 D. Liventsev,²⁴ R. Louvot,³² J. MacNaughton,¹³ D. Marlow,⁵³ D. Matvienko,² S. McOnie,⁶¹
 Y. Mikami,⁶⁶ M. Nayak,¹⁷ K. Miyabayashi,⁴⁰ Y. Miyachi,^{54, 74} H. Miyata,⁴⁶ Y. Miyazaki,³⁸
 R. Mizuk,²⁴ G. B. Mohanty,⁶² D. Mohapatra,⁷² A. Moll,^{36, 63} T. Mori,³⁸ T. Müller,²⁷
 N. Muramatsu,^{54, 49} R. Mussa,²³ T. Nagamine,⁶⁶ Y. Nagasaka,¹⁴ Y. Nakahama,⁶⁷
 I. Nakamura,¹³ E. Nakano,⁴⁸ T. Nakano,^{54, 49} M. Nakao,¹³ H. Nakayama,¹³ H. Nakazawa,⁴¹

Z. Natkaniec,⁴⁴ E. Nedelkovska,³⁶ K. Neichi,⁶⁵ S. Neubauer,²⁷ C. Ng,⁶⁷ M. Niiyama,^{54, 30}
 S. Nishida,¹³ K. Nishimura,¹² O. Nitoh,⁷⁰ S. Noguchi,⁴⁰ T. Nozaki,¹³ A. Ogawa,⁵⁵
 S. Ogawa,⁶⁴ T. Ohshima,³⁸ S. Okuno,²⁶ S. L. Olsen,^{58, 12} Y. Onuki,⁶⁶ W. Ostrowicz,⁴⁴
 H. Ozaki,¹³ P. Pakhlov,²⁴ G. Pakhlova,²⁴ H. Palka,^{44, *} C. W. Park,⁶⁰ H. Park,³¹
 H. K. Park,³¹ K. S. Park,⁶⁰ L. S. Peak,⁶¹ T. K. Pedlar,³⁴ T. Peng,⁵⁷ R. Pestotnik,²⁵
 M. Peters,¹² M. Petrič,²⁵ L. E. Piilonen,⁷² A. Poluektov,² M. Prim,²⁷ K. Prothmann,^{36, 63}
 B. Reisert,³⁶ M. Ritter,³⁶ M. Röhrken,²⁷ J. Rorie,¹² M. Rozanska,⁴⁴ S. Ryu,⁵⁸ H. Sahoo,¹²
 K. Sakai,¹³ Y. Sakai,¹³ D. Santel,⁵ N. Sasao,³⁰ O. Schneider,³² P. Schönmeier,⁶⁶
 C. Schwanda,²⁰ A. J. Schwartz,⁵ R. Seidl,⁵⁵ A. Sekiya,⁴⁰ K. Senyo,³⁸ O. Seon,³⁸
 M. E. Sevior,³⁷ L. Shang,¹⁹ M. Shapkin,²¹ V. Shebalin,² C. P. Shen,¹² T.-A. Shibata,^{54, 68}
 H. Shibuya,⁶⁴ S. Shinomiya,⁴⁹ J.-G. Shiu,⁴³ B. Shwartz,² A. L. Sibidanov,⁶¹ F. Simon,^{36, 63}
 J. B. Singh,⁵¹ R. Sinha,²² P. Smerkol,²⁵ Y.-S. Sohn,⁷⁵ A. Sokolov,²¹ E. Solovieva,²⁴
 S. Stanič,⁴⁷ M. Starič,²⁵ J. Stypula,⁴⁴ S. Sugihara,⁶⁷ A. Sugiyama,⁵⁶ M. Sumihama,^{54, 8}
 K. Sumisawa,¹³ T. Sumiyoshi,⁶⁹ K. Suzuki,³⁸ S. Suzuki,⁵⁶ S. Y. Suzuki,¹³ H. Takeichi,³⁸
 M. Tanaka,¹³ S. Tanaka,¹³ N. Taniguchi,¹³ G. Tatishvili,⁵⁰ G. N. Taylor,³⁷ Y. Teramoto,⁴⁸
 I. Tikhomirov,²⁴ K. Trabelsi,¹³ Y. F. Tse,³⁷ T. Tsuboyama,¹³ Y.-W. Tung,⁴³
 M. Uchida,^{54, 68} T. Uchida,¹³ Y. Uchida,⁹ S. Uehara,¹³ K. Ueno,⁴³ T. Uglov,²⁴
 M. Ullrich,⁷ Y. Unno,¹¹ S. Uno,¹³ P. Urquijo,¹ Y. Ushiroda,¹³ Y. Usov,² S. E. Vahsen,¹²
 P. Vanhoefer,³⁶ G. Varner,¹² K. E. Varvell,⁶¹ K. Vervink,³² A. Vinokurova,² A. Vossen,¹⁸
 C. H. Wang,⁴² J. Wang,⁵² M.-Z. Wang,⁴³ P. Wang,¹⁹ X. L. Wang,¹⁹ M. Watanabe,⁴⁶
 Y. Watanabe,²⁶ R. Wedd,³⁷ M. Werner,⁷ E. White,⁵ J. Wicht,¹³ L. Widhalm,²⁰
 J. Wiechczynski,⁴⁴ K. M. Williams,⁷² E. Won,²⁹ T.-Y. Wu,⁴³ B. D. Yabsley,⁶¹
 H. Yamamoto,⁶⁶ J. Yamaoka,¹² Y. Yamashita,⁴⁵ M. Yamauchi,¹³ C. Z. Yuan,¹⁹ Y. Yusa,⁴⁶
 D. Zander,²⁷ C. C. Zhang,¹⁹ L. M. Zhang,⁵⁷ Z. P. Zhang,⁵⁷ L. Zhao,⁵⁷ V. Zhilich,²
 P. Zhou,⁷³ V. Zhulanov,² T. Zivko,²⁵ A. Zupanc,²⁷ N. Zwahlen,³² and O. Zyukova²

(The Belle Collaboration)

¹*University of Bonn, Bonn*

²*Budker Institute of Nuclear Physics SB RAS and
Novosibirsk State University, Novosibirsk 630090*

³*Faculty of Mathematics and Physics, Charles University, Prague*

⁴*Chiba University, Chiba*

⁵*University of Cincinnati, Cincinnati, Ohio 45221*

⁶*Department of Physics, Fu Jen Catholic University, Taipei*

⁷*Justus-Liebig-Universität Gießen, Gießen*

⁸*Gifu University, Gifu*

⁹*The Graduate University for Advanced Studies, Hayama*

¹⁰*Gyeongsang National University, Chinju*

¹¹*Hanyang University, Seoul*

¹²*University of Hawaii, Honolulu, Hawaii 96822*

¹³*High Energy Accelerator Research Organization (KEK), Tsukuba*

¹⁴*Hiroshima Institute of Technology, Hiroshima*

¹⁵*University of Illinois at Urbana-Champaign, Urbana, Illinois 61801*

¹⁶*Indian Institute of Technology Guwahati, Guwahati*

¹⁷*Indian Institute of Technology Madras, Madras*

¹⁸*Indiana University, Bloomington, Indiana 47408*

¹⁹*Institute of High Energy Physics,*

Chinese Academy of Sciences, Beijing

²⁰*Institute of High Energy Physics, Vienna*

²¹*Institute of High Energy Physics, Protvino*

²²*Institute of Mathematical Sciences, Chennai*

²³*INFN - Sezione di Torino, Torino*

²⁴*Institute for Theoretical and Experimental Physics, Moscow*

²⁵*J. Stefan Institute, Ljubljana*

²⁶*Kanagawa University, Yokohama*

²⁷*Institut für Experimentelle Kernphysik,*

Karlsruher Institut für Technologie, Karlsruhe

²⁸*Korea Institute of Science and Technology Information, Daejeon*

²⁹*Korea University, Seoul*

³⁰*Kyoto University, Kyoto*

³¹*Kyungpook National University, Taegu*

³²*École Polytechnique Fédérale de Lausanne (EPFL), Lausanne*

³³*Faculty of Mathematics and Physics, University of Ljubljana, Ljubljana*

- ³⁴*Luther College, Decorah, Iowa 52101*
- ³⁵*University of Maribor, Maribor*
- ³⁶*Max-Planck-Institut für Physik, München*
- ³⁷*University of Melbourne, School of Physics, Victoria 3010*
- ³⁸*Nagoya University, Nagoya*
- ³⁹*Nara University of Education, Nara*
- ⁴⁰*Nara Women's University, Nara*
- ⁴¹*National Central University, Chung-li*
- ⁴²*National United University, Miao Li*
- ⁴³*Department of Physics, National Taiwan University, Taipei*
- ⁴⁴*H. Niewodniczanski Institute of Nuclear Physics, Krakow*
- ⁴⁵*Nippon Dental University, Niigata*
- ⁴⁶*Niigata University, Niigata*
- ⁴⁷*University of Nova Gorica, Nova Gorica*
- ⁴⁸*Osaka City University, Osaka*
- ⁴⁹*Osaka University, Osaka*
- ⁵⁰*Pacific Northwest National Laboratory, Richland, Washington 99352*
- ⁵¹*Panjab University, Chandigarh*
- ⁵²*Peking University, Beijing*
- ⁵³*Princeton University, Princeton, New Jersey 08544*
- ⁵⁴*Research Center for Nuclear Physics, Osaka*
- ⁵⁵*RIKEN BNL Research Center, Upton, New York 11973*
- ⁵⁶*Saga University, Saga*
- ⁵⁷*University of Science and Technology of China, Hefei*
- ⁵⁸*Seoul National University, Seoul*
- ⁵⁹*Shinshu University, Nagano*
- ⁶⁰*Sungkyunkwan University, Suwon*
- ⁶¹*School of Physics, University of Sydney, NSW 2006*
- ⁶²*Tata Institute of Fundamental Research, Mumbai*
- ⁶³*Excellence Cluster Universe, Technische Universität München, Garching*
- ⁶⁴*Toho University, Funabashi*
- ⁶⁵*Tohoku Gakuin University, Tagajo*

⁶⁶*Tohoku University, Sendai*

⁶⁷*Department of Physics, University of Tokyo, Tokyo*

⁶⁸*Tokyo Institute of Technology, Tokyo*

⁶⁹*Tokyo Metropolitan University, Tokyo*

⁷⁰*Tokyo University of Agriculture and Technology, Tokyo*

⁷¹*Toyama National College of Maritime Technology, Toyama*

⁷²*CNP, Virginia Polytechnic Institute and State University, Blacksburg, Virginia 24061*

⁷³*Wayne State University, Detroit, Michigan 48202*

⁷⁴*Yamagata University, Yamagata*

⁷⁵*Yonsei University, Seoul*

(Dated: November 5, 2018)

Abstract

We report the first observation of the radiative transition $h_b(1P) \rightarrow \eta_b(1S)\gamma$, where the $h_b(1P)$ is produced in $\Upsilon(5S) \rightarrow h_b(1P)\pi^+\pi^-$ dipion transitions. We measure the $\eta_b(1S)$ mass to be $(9401.0 \pm 1.9^{+1.4}_{-2.4}) \text{ MeV}/c^2$ with a width of $(12.4^{+5.5+11.5}_{-4.6-3.4}) \text{ MeV}$ and a decay branching fraction of $\mathcal{B}[h_b(1P) \rightarrow \eta_b(1S)\gamma] = (49.8 \pm 6.8^{+10.9}_{-5.2})\%$. The measured $\eta_b(1S)$ mass corresponds to a hyperfine splitting of $(59.3 \pm 1.9^{+2.4}_{-1.4}) \text{ MeV}/c^2$. This value deviates significantly from the current world average obtained from measurements of $\Upsilon(3S) \rightarrow \eta_b(1S)\gamma$ and $\Upsilon(2S) \rightarrow \eta_b(1S)\gamma$ reactions. We also report updated results for the $h_b(1P)$ mass $(9899.0 \pm 0.4 \pm 1.0) \text{ MeV}/c^2$ and its hyperfine splitting $(0.8 \pm 1.1) \text{ MeV}/c^2$. These measurements are performed using a 121.4 fb^{-1} data sample collected at the peak of the $\Upsilon(5S)$ resonance with the Belle detector at the KEKB asymmetric-energy e^+e^- collider.

PACS numbers: 14.40.Pq, 13.25.Gv, 12.39.Pn

INTRODUCTION

Recently Belle reported the first observation of the $h_b(1P)$ and $h_b(2P)$ states [1]. The radiative transition to the $\eta_b(1S)$ is expected to be one of the dominant decay modes of the $h_b(1P)$: $ggg/\eta_b(1S)\gamma/gg\gamma = 57/41/2\%$ [2]. Belle's large $h_b(1P)$ sample provide an opportunity to study the $\eta_b(1S)$, which is the ground state of the bottomonium system with $b\bar{b}$ spin and orbital angular momentum equal to zero. The hyperfine splitting defined as $\Delta M_{\text{HF}}[\eta_b(1S)] = M[\Upsilon(1S)] - M[\eta_b(1S)]$ provides a test of spin-spin interactions [3]. The $\eta_b(1S)$ was first observed by BaBar [4, 5] and confirmed by CLEO [6]. Its mass is found to be higher than theoretical predictions [7, 8]. The tension between experimental results and predictions strongly motivates further experimental studies of the $\eta_b(1S)$. We note that no experimental information is available on the $\eta_b(1S)$ width.

We report the first observation of the radiative transition $h_b(1P) \rightarrow \eta_b(1S)\gamma$ and measurements of the $\eta_b(1S)$ mass, width and decay branching fraction. We use a 121.4 fb^{-1} data sample collected at the peak of the $\Upsilon(5S)$ resonance ($\sqrt{s} \sim 10.865 \text{ GeV}$) with the Belle detector [9] at the KEKB asymmetric-energy e^+e^- collider [10].

METHOD

In the decay chain $\Upsilon(5S) \rightarrow Z_b^+\pi^-, Z_b^+ \rightarrow h_b(1P)\pi^+, h_b(1P) \rightarrow \eta_b(1S)\gamma$ we reconstruct only the π^- , π^+ and γ . Here Z_b^+ denotes the $Z_b(10610)^+$ and $Z_b(10650)^+$, the two charged bottomonium-like resonances first identified by Belle in Ref. [11]. In this decay the typical momenta of the π^- , π^+ and γ are $240 \text{ MeV}/c$, $730 \text{ MeV}/c$ and $500 \text{ MeV}/c$, respectively.

We define the missing mass of X (where $X = \pi^+\pi^-$ or $\pi^+\pi^-\gamma$) as

$$M_{\text{miss}}(X) = \sqrt{(E_{\text{c.m.}} - E_X^*)^2 - p_X^{*2}}, \quad (1)$$

where $E_{\text{c.m.}}$ is the center-of-mass (c.m.) energy and E_X^* and p_X^* are the energy and momentum of the X system measured in the c.m. frame.

The $\pi^+\pi^-\gamma$ combinations from the signal decay chain form a cluster in the $M_{\text{miss}}(\pi^+\pi^-\gamma)$ versus $M_{\text{miss}}(\pi^+\pi^-)$ plane centered at $M[\eta_b(1S)]$ and $M[h_b(1P)]$, respectively (see Fig. 1). In this plane there is a vertical band due to correctly reconstructed $\pi^+\pi^-$ combinations and misreconstructed γ 's, and a slanted band due to correctly reconstructed γ 's and misreconstructed $\pi^+\pi^-$. We introduce a new variable $\Delta M_{\text{miss}}(\pi^+\pi^-\gamma) \equiv M_{\text{miss}}(\pi^+\pi^-\gamma) -$

$M_{\text{miss}}(\pi^+\pi^-) + m[h_b(1P)]$. The advantage of the new variable is that the band with correctly reconstructed γ 's and misreconstructed $\pi^+\pi^-$ combinations becomes horizontal (see Fig. 1) and the variables $\Delta M_{\text{miss}}(\pi^+\pi^-\gamma)$ and $M_{\text{miss}}(\pi^+\pi^-)$ are not correlated for signal events.

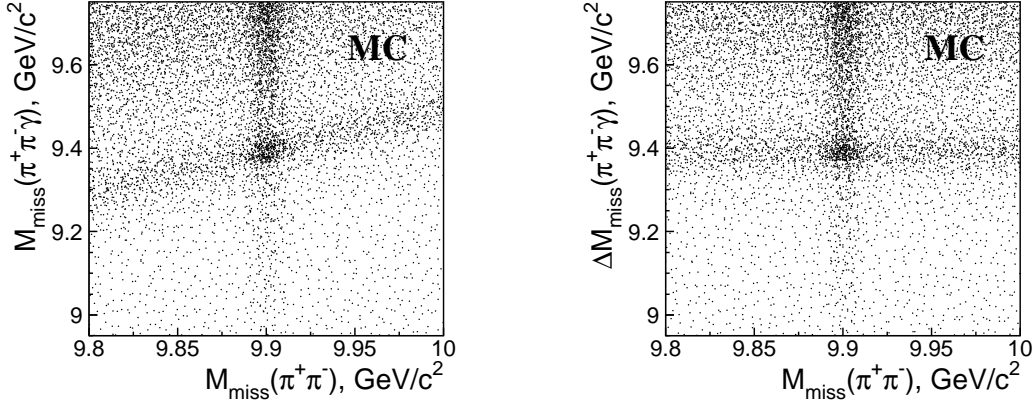


FIG. 1: Results of Monte-Carlo simulation for signal $h_b(1P) \rightarrow \eta_b(1S)\gamma$ transitions. $M_{\text{miss}}(\pi^+\pi^-\gamma)$ vs. $M_{\text{miss}}(\pi^+\pi^-)$ distribution (left) and $\Delta M_{\text{miss}}(\pi^+\pi^-\gamma)$ vs. $M_{\text{miss}}(\pi^+\pi^-)$ distribution (right) for all $\pi^+\pi^-\gamma$ combinations in the event.

It may be possible to perform a two dimensional fit to the $\Delta M_{\text{miss}}(\pi^+\pi^-\gamma)$ vs. $M_{\text{miss}}(\pi^+\pi^-)$ distribution. However, we follow a more intuitive approach. We divide the $\Delta M_{\text{miss}}(\pi^+\pi^-\gamma)$ vs. $M_{\text{miss}}(\pi^+\pi^-)$ plane into $10 \text{ MeV}/c^2$ wide horizontal slices, project each slice onto the $M_{\text{miss}}(\pi^+\pi^-)$ axis and fit the $M_{\text{miss}}(\pi^+\pi^-)$ distribution. We thus find the dependence of the $h_b(1P)$ yield on the $\Delta M_{\text{miss}}(\pi^+\pi^-\gamma)$ variable. We then search for the $\eta_b(1S)$ signal as a peak in this distribution.

SELECTION

We start with hadron event selection [12]. Continuum $e^+e^- \rightarrow q\bar{q}$ ($q = u, d, s, c$) background is suppressed by requiring that the ratio of the second to zeroth Fox-Wolfram moments satisfies $R_2 < 0.3$ [13]. The $\pi^+\pi^-$ selection requirements are the same as in the $h_b(1P)$ and $h_b(2P)$ observation paper [1]. We consider all positively identified $\pi^+\pi^-$ pairs that originate from the vicinity of the interaction point. We require that the $h_b(1P)$ is produced via an intermediate Z_b , $10.59 \text{ MeV}/c^2 < M_{\text{miss}}(\pi) < 10.67 \text{ MeV}/c^2$ [11]. This

requirement significantly reduces the background (by a factor of 5.2) without any significant loss of the signal. We consider all γ candidates, and apply a π^0 veto, $|M(\gamma\gamma_2) - m_{\pi^0}| > 13 \text{ MeV}/c^2$ with $E_{\gamma_2} > 75 \text{ MeV}$, where γ_2 is any photon candidate in the event. The values of the cuts were optimized based on the figure of merit $\text{FoM} = \frac{S}{\sqrt{B}}$, where S is the number of signal events in the signal Monte-Carlo (MC), B is the number of background events estimated from a small fraction (0.1%) of data.

STUDY OF INCLUSIVE $h_b(1P)$ SIGNAL

The fit to the inclusive $M_{\text{miss}}(\pi^+\pi^-)$ spectrum (before combining $\pi^+\pi^-$ and γ candidates) with the requirement of the intermediate Z_b is shown in Fig. 2. We use the same fit procedure

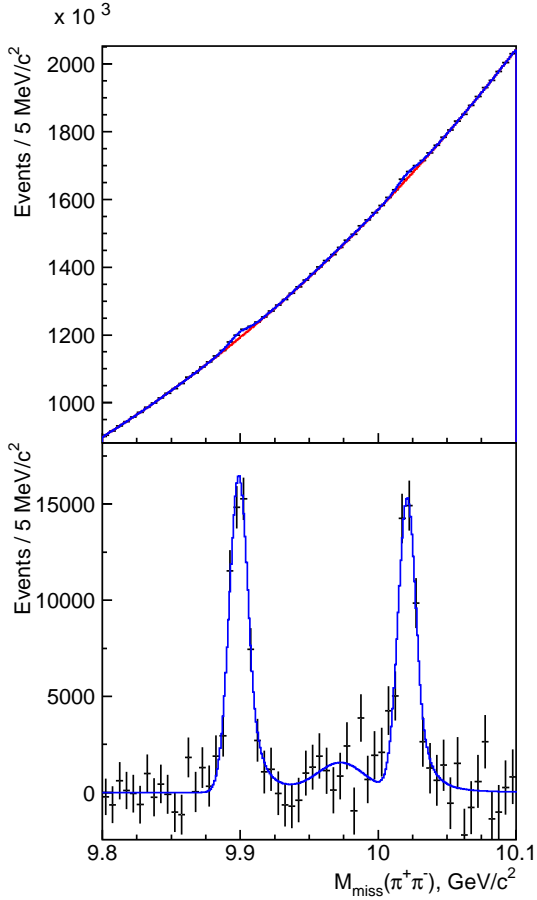


FIG. 2: $M_{\text{miss}}(\pi^+\pi^-)$ spectrum with the requirement of an intermediate Z_b (top) and residuals (bottom).

as in Ref. [1]. The fit function consists of four components: the $h_b(1P)$ signal, the $\Upsilon(2S)$

signal, a reflection from the $\Upsilon(3S) \rightarrow \Upsilon(1S)\pi^+\pi^-$ decay, and combinatorial background. The shapes of the peaking components are determined from the analysis of the $\mu^+\mu^-\pi^+\pi^-$ data sample, that contains the $\Upsilon(nS) \rightarrow \mu^+\mu^-$ ($n = 1, 2, 3$) decays. The signals are found to have tails that account for about 8% of the yield and are due to the initial state radiation of soft photons. The $h_b(1P)$ and $\Upsilon(2S)$ intrinsic widths are negligible compared to the detector resolution, therefore the signals are described by a Crystal Ball function with width $\sigma = 6.5 \text{ MeV}/c^2$ and $6.8 \text{ MeV}/c^2$, respectively. The width (σ) of the $h_b(1P)$ signal is determined from linear interpolation in mass from the widths of the $\Upsilon(nS)$ peaks. The tail parameters of the $h_b(1P)$ signal are assumed to be the same as for the $\Upsilon(2S)$ signal. The $\Upsilon(3S) \rightarrow \Upsilon(1S)\pi^+\pi^-$ reflection is described by a single Gaussian function with a width of $\sigma = 18 \text{ MeV}$. The combinatorial background is parameterized by a third order Chebyshev polynomial. We perform binned χ^2 fit using $1 \text{ MeV}/c^2$ bins, though for clarity we display the data in $5 \text{ MeV}/c^2$ bins. The results of the fit are given in Table I. The confidence level of this fit is 56%.

TABLE I: The yield and mass of the $h_b(1P)$ from the fit to the inclusive $M_{\text{miss}}(\pi^+\pi^-)$ spectrum.

	Yield, 10^3	Mass, MeV/c^2
$h_b(1P)$	$(61.3 \pm 3.1^{+2.2}_{-0.3}) \times 10^3$	$(9899.0 \pm 0.4 \pm 1.0) \text{ MeV}/c^2$
$\Upsilon(3S) \rightarrow \Upsilon(1S)$	$(13 \pm 7) \times 10^3$	$9973.0 \text{ MeV}/c^2$
$\Upsilon(2S)$	$(54.8 \pm 3.9) \times 10^3$	$(10021.1 \pm 0.5) \text{ MeV}/c^2$

To estimate systematic uncertainty on the $h_b(1P)$ parameters we vary the Chebyshev polynomial order (+1, +2); and fit range (we reduce it to $9.98 \text{ MeV}/c^2$ and exclude all peaking components except for the $h_b(1P)$ signal). We also introduce a correction factor for the signal width and allow it to float (we find $f = 0.99 \pm 0.07$). We use a signal tail shape not only from the $\Upsilon(2S)$ (the default case), but also from the $\Upsilon(1S)$ and $\Upsilon(3S)$. A summary of the systematic uncertainties is given in Table II. For the mass measurement we introduce an additional $\pm 1 \text{ MeV}/c^2$ uncertainty due to possible local variations of background shape as estimated in Ref. [1] using deviations of reference channels from the PDG values. The new value for the $h_b(1P)$ mass corresponds to a hyperfine splitting $\Delta M_{\text{HF}}[h_b(1P)] = (0.8 \pm 1.1) \text{ MeV}/c^2$, where statistical and systematic uncertainties are added in quadrature.

TABLE II: Systematic uncertainties in the $h_b(1P)$ parameters from various sources.

	Polynomial	Fit	Signal
	order	range	shape
$N[h_b(1P)], 10^3$	$\begin{array}{c} +1.8 \\ -0 \end{array}$	$\begin{array}{c} +1.1 \\ -0 \end{array}$	$\begin{array}{c} +0.5 \\ -0.3 \end{array}$
$M[h_b(1P)], \text{MeV}/c^2$	$\begin{array}{c} +0.1 \\ -0 \end{array}$	$\begin{array}{c} +0.1 \\ -0 \end{array}$	$\begin{array}{c} +0 \\ -0.1 \end{array}$

EXTRACTION OF $\eta_b(1S)$ SIGNAL

To extract the $\eta_b(1S)$ signal we fit the $M_{\text{miss}}(\pi^+\pi^-)$ spectra in the $\Delta M_{\text{miss}}(\pi^+\pi^-\gamma)$ bins. In the fit function we fix the masses of signals at the values given in Table I. We use a $10 \text{ MeV}/c^2$ bin size in $\Delta M_{\text{miss}}(\pi^+\pi^-\gamma)$. The results for the $h_b(1P)$, $\Upsilon(2S)$ and $\Upsilon(3S) \rightarrow \Upsilon(1S)$ reflection yields as a function of the $\Delta M_{\text{miss}}(\pi^+\pi^-\gamma)$ are shown in Fig. 3. The $h_b(1P)$ distribution shows a clear peak at $9.4 \text{ GeV}/c^2$ that we identify as the $\eta_b(1S)$ signal, while the other distributions do not exhibit significant structures.

We search for peaking backgrounds in the $\Delta M_{\text{miss}}(\pi^+\pi^-\gamma)$ distribution of the $h_b(1P)$ yield. We use a MC simulation for generic $\Upsilon(5S)$ decays and consider separately $h_b(1P) \rightarrow ggg$, $h_b(1P) \rightarrow gg\gamma$ and $e^+e^- \rightarrow \gamma_{ISR}\Upsilon(3S)$ processes. We do not find any sources of peaking background.

CALIBRATION

We use the $B^+ \rightarrow \chi_{c1}K^+$, $\chi_{c1} \rightarrow J/\psi\gamma$, $J/\psi \rightarrow e^+e^-/\mu^+\mu^-$ data sample for calibration. We require that the kaon and lepton candidates are positively identified and originate from the vicinity of the IP. For the $J/\psi \rightarrow e^+e^-$ mode we attempt to reconstruct and recover bremsstrahlung photons. The mass window around the nominal J/ψ mass is $\pm 30 \text{ MeV}/c^2$ ($\pm 50 \text{ MeV}/c^2$) for the $\mu^+\mu^-$ (e^+e^-) mode. We perform a mass constrained fit to the J/ψ and χ_{c1} candidates. We require $|\Delta E| < 30 \text{ MeV}$ and $M_{bc} > 5.27 \text{ MeV}/c^2$, which are loose requirements. The ΔE sidebands are defined as $40 < |\Delta E| < 100 \text{ MeV}$. The background is efficiently suppressed by the requirement $\cos\theta_\gamma > -0.2$, where θ_γ is the helicity angle of the χ_{c1} defined as the angle between the γ momentum and χ_{c1} boost direction in the χ_{c1} rest frame. The particular value of the cut is chosen so that the average γ energy in the c.m. frame is $500 \text{ MeV}/c^2$, i.e. is equal to the average energy of the photon in the $h_b(1P) \rightarrow \eta_b(1S)$

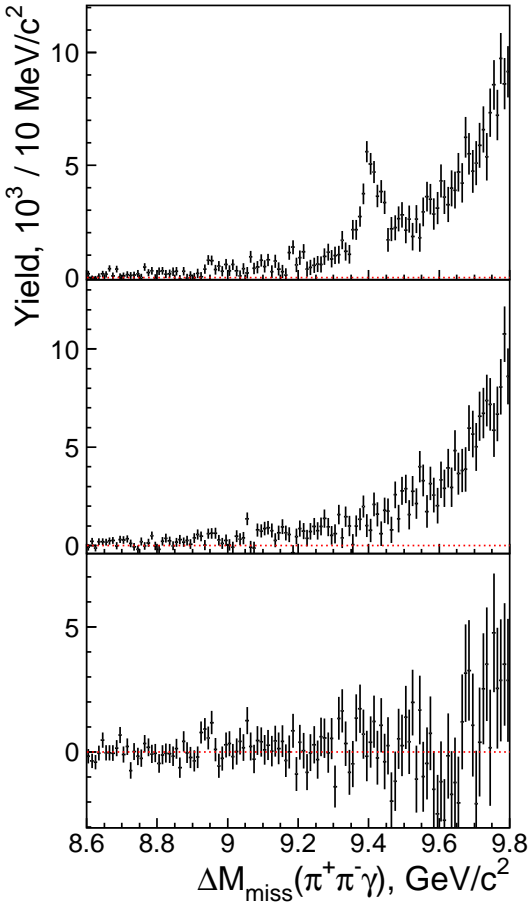


FIG. 3: The results for the $h_b(1P)$ (top), $\Upsilon(2S)$ (middle) and $\Upsilon(3S) \rightarrow \Upsilon(1S)$ reflection (bottom) yields as a function of $\Delta M_{\text{miss}}(\pi^+\pi^-\gamma)$.

transition. The ΔE distribution with the requirement $3.44 < M(J/\psi\gamma) < 3.54 \text{ GeV}/c^2$ and $M(J/\psi\gamma)$ distribution for the ΔE signal region and for the normalized sidebands (see Fig. 4) indicate, that the background is small.

We parameterize the $J/\psi\gamma$ mass distribution in MC by a Crystal Ball function [14] with an asymmetric core and with tails on both sides (8 parameters in total). This parameterization describes MC reasonably well (see Fig. 5). For the core we find $\sigma_1 = 11.9 \text{ MeV}/c^2$ (left side) and $\sigma_2 = 6.8 \text{ MeV}/c^2$ (right side).

We fit the $M(J/\psi\gamma)$ distribution in data fixing the σ_1 and σ_2 parameters and introducing a shift of the peak position and width correction factor (see Fig. 5). We find for the shift: $-0.7 \pm 0.3^{+0.2}_{-0.4} \text{ MeV}/c^2$ and for the width correction factor: $1.15 \pm 0.06^{+0.05}_{-0.06}$. The systematic uncertainty is estimated (1) by varying the fit interval; (2) by using only the left normalized

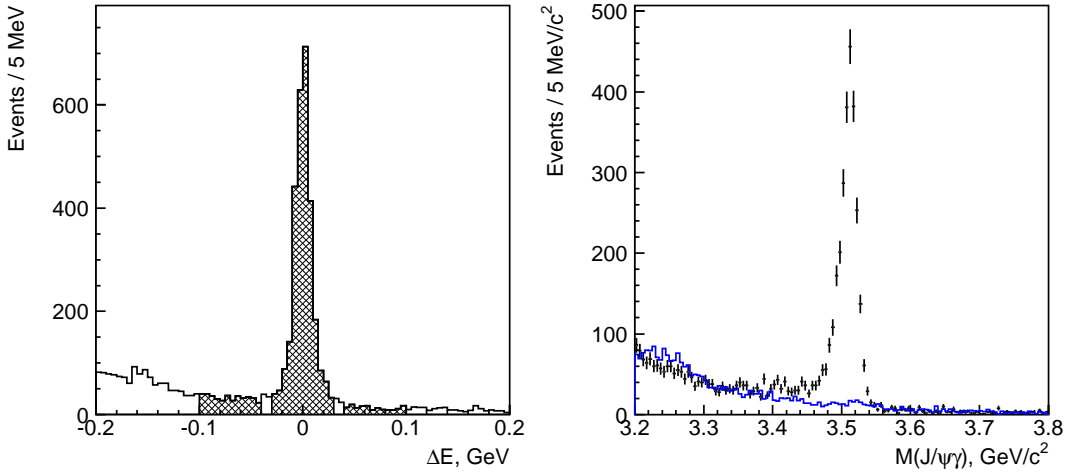


FIG. 4: (Left) ΔE distribution for the selected $B^+ \rightarrow \chi_{c1} K^+$ decay candidates; signal and sidebands regions are hatched. (Right) $M(J/\psi\gamma)$ distribution for the ΔE signal region (points with error bars) and for the normalized sidebands (open blue histogram).

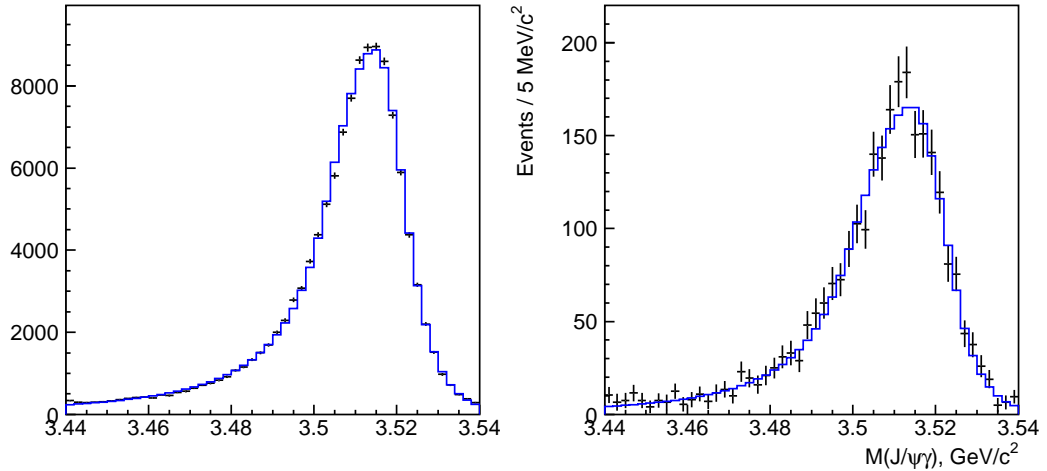


FIG. 5: The $M(J/\psi\gamma)$ distribution in MC (left) and data ΔE signal region with ΔE sidebands subtracted (right). The fit is described in the text.

ΔE sideband for subtraction or only the right sideband; (3) by varying the σ_1/σ_2 ratio in the parameterization: we use the σ_1/σ_2 ratio from the fit to the distribution in (i) data and (ii) in the $h_b(1P) \rightarrow \eta_b(1S)\gamma$ MC.

$\eta_b(1S)$ MASS AND WIDTH

We fit the $\Delta M_{\text{miss}}(\pi^+\pi^-\gamma)$ distribution to a sum of an $\eta_b(1S)$ signal component and a combinatorial background contribution (see Fig. 6). The signal is a non-relativistic Breit-

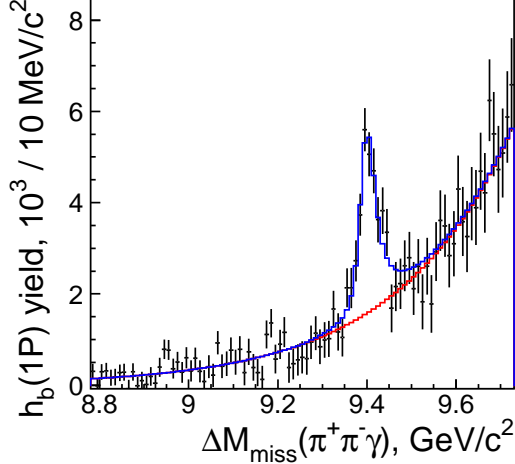


FIG. 6: $\Delta M_{\text{miss}}(\pi^+\pi^-\gamma)$ distribution of the $h_b(1P)$ yield with fit result superimposed.

Wigner (this parameterization is chosen to simplify comparison with BaBar and CLEO results) convolved with the calibrated resolution function (we use the shift and width correction factor determined from the χ_{c1} signal in data). The combinatorial background is parameterized by an exponential function. We verify the fit procedure using MC. The fit results are shown in Table III. The confidence level of the fit is 77%. The significance of the

TABLE III: The yield, mass and width of the $\eta_b(1S)$ signal from the fit to the $\Delta M_{\text{miss}}(\pi^+\pi^-\gamma)$ distribution of the $h_b(1P)$ yield.

$N[\eta_b(1S)]$	$(21.9 \pm 2.0^{+5.6}_{-1.7}) \times 10^3$
$M[\eta_b(1S)]$	$(9401.0 \pm 1.9^{+1.4}_{-2.4}) \text{ MeV}/c^2$
$\Gamma[\eta_b(1S)]$	$(12.4^{+5.5+11.5}_{-4.6-3.4}) \text{ MeV}$

$\eta_b(1S)$ signal is 14σ .

To estimate the systematic uncertainty we vary the fit range in the fits to the $M_{\text{miss}}(\pi^+\pi^-)$ distributions (instead of the default range $9.8 - 10.1 \text{ GeV}/c^2$ we use $9.8 - 9.98 \text{ GeV}/c^2$); we also vary the polynomial order in these fits (we increase the order by one and by two); we

vary the binning of the $\Delta M_{\text{miss}}(\pi^+\pi^-\gamma)$ distribution (we scan the starting point of bin with $1 \text{ MeV}/c^2$ steps); we also vary the fit range in the fits to the $\Delta M_{\text{miss}}(\pi^+\pi^-\gamma)$ distribution; we vary the parameterization of the combinatorial background in the fits to the $\Delta M_{\text{miss}}(\pi^+\pi^-\gamma)$ distribution (in addition to a single exponential we use the sum of two exponentials, second and third order polynomials, we also use the function $\exp(\sum_{k=0}^n c_k x^k)$, i.e. an exponential of a polynomial, with $n = 2, 3, 4$); to take into account the uncertainty in the resolution function we vary the width correction factor by $\pm 1\sigma$ (we combine its statistical and systematic uncertainty in quadrature) and we take into account the uncertainty in the mass shift parameter; we vary the selection criteria [R_2 cuts: 0.25, 0.3 (default), 0.35, 0.4; π^0 veto, cut on $|M(\gamma\gamma_2) - M_{\pi^0}|$: 10, 13 (default), 15 MeV/c^2 , cut on $E_{\gamma 2}$: 50, 75 (default), 100 MeV]; we take into account the uncertainty in the $h_b(1P)$ mass. A summary of the systematic uncertainties is given in Table IV. To obtain the total systematic uncertainty we add all

TABLE IV: Systematic uncertainties in the $\eta_b(1S)$ parameters from various sources.

	$N[\eta_b(1S)], 10^3$	$M[\eta_b(1S)], \text{MeV}/c^2$	$\Gamma[\eta_b(1S)], \text{MeV}$
Range in $M_{\text{miss}}(\pi^+\pi^-)$ fits	+0.0 -0.6	+0.0 -0.2	+0.0 -0.1
Poly order in $M_{\text{miss}}(\pi^+\pi^-)$ fits	+0.0 -0.6	+0.1 -0.1	+0.0 -0.4
$\Delta M_{\text{miss}}(\pi^+\pi^-\gamma)$ binning	+0.2 -0.1	+0.3 -0.8	+1.0 -0.8
Range in $\Delta M_{\text{miss}}(\pi^+\pi^-\gamma)$ fits	+0.9 -0.2	+0.1 -0.1	+1.4 -0.3
$\Delta M_{\text{miss}}(\pi^+\pi^-\gamma)$ bg parameterization	+5.5 -1.4	+0.5 -0.2	+10.9 -2.2
Resolution function	+0.2 -0.1	+0.5 -0.5	+1.4 -1.4
Selection requirements	-	+0.4 -1.9	+3.0 -2.0
$h_b(1P)$ mass	-	+1.1 -1.1	-
Total	+5.6 -1.7	+1.4 -2.4	+11.5 -3.4

sources in quadrature.

We study the shift of the $\eta_b(1S)$ parameters in case other line-shape parameterizations are used. We consider the KEDR parameterization [15]: $BW(m) \frac{E^3 E_0^2}{EE_0 + (E-E_0)^2}$, where $BW(m)$ is the Breit-Wigner function, E [E_0] is the γ energy in the $h_b(1P)$ rest frame [calculated for the pole mass of the $\eta_b(1S)$]. We also consider the CLEO parameterization [16]: $BW(m) E^3 \exp(-\frac{E^2}{8\beta^2})$, where β is a fit parameter. Both the KEDR and CLEO Collaborations used these parameterizations for the $J/\psi \rightarrow \eta_c \gamma$ transitions. We do not find

considerable shifts in the $\eta_b(1S)$ yield, mass or width if these alternative parameterizations are used instead of the non-relativistic Breit-Wigner function.

The significance of the $\eta_b(1S)$ signal including systematic uncertainties is 13σ .

MEASUREMENT OF $\mathcal{B}[h_b(1P) \rightarrow \eta_b(1S)\gamma]$

We measure the $\eta_b(1S)$ [$h_b(1P)$] yield in the events that fail the $R_2 < 0.3$ or π^0 veto requirements [$R_2 < 0.3$ requirement]. In the fit to the $\Delta M_{\text{miss}}(\pi^+\pi^-\gamma)$ [$M_{\text{miss}}(\pi^+\pi^-)$] distribution for the rejected events we allow the $\eta_b(1S)$ mass and width [the $h_b(1P)$ mass] to float within the uncertainties of the measured values given in Table III (Table I). We find $N_1[\eta_b(1S)] = (5.5 \pm 2.7 \pm 2.1) \times 10^3$ and $N_1[h_b(1P)] = (13.0 \pm 2.8 \pm 0.5) \times 10^3$.

From the N_1 values and the yields from Tables I and III we determine the total yields $N_0[h_b(1P)]$ and $N_0[\eta_b(1S)]$ without requirements on R_2 or a π^0 veto. We obtain $\mathcal{B} = N_0[\eta_b(1S)]/N_0[h_b(1P)]/\epsilon$, where ϵ is the reconstruction efficiency of the radiative photon, which is found from MC to be 74.1% with 2% systematic uncertainty (the MC statistical uncertainty is negligible). We find

$$\mathcal{B}[h_b(1P) \rightarrow \eta_b(1S)\gamma] = (49.8 \pm 6.8^{+10.9}_{-5.2})\%.$$

CONCLUSIONS

We report the first observation of the radiative transition $h_b(1P) \rightarrow \eta_b(1S)\gamma$, where the $h_b(1P)$ is produced in $\Upsilon(5S) \rightarrow h_b(1P)\pi^+\pi^-$ dipion transitions. We report the single most precise measurement of the $\eta_b(1S)$ mass, $(9401.0 \pm 1.9^{+1.4}_{-2.4}) \text{ MeV}/c^2$, which corresponds to the hyperfine splitting $\Delta M_{\text{HF}}[\eta_b(1S)] = (59.3 \pm 1.9^{+2.4}_{-1.4}) \text{ MeV}/c^2$. This value deviates significantly from the current world average [17] but decreases tension with theoretical expectations [7, 8] (see Fig. 7). We report the first measurement of the $\eta_b(1S)$ width $(12.4^{+5.5+11.5}_{-4.6-3.4}) \text{ MeV}$, which is in the middle of the range of predictions from potential models, 4 – 20 MeV [18]. For the branching fraction we find $\mathcal{B}[h_b(1P) \rightarrow \eta_b(1S)\gamma] = (49.8 \pm 6.8^{+10.9}_{-5.2})\%$ in agreement with expectations [2].

We also report updated results for the $h_b(1P)$ mass $(9899.0 \pm 0.4 \pm 1.0) \text{ MeV}/c^2$ and hyper-fine splitting $\Delta M_{\text{HF}}[h_b(1P)] = (0.8 \pm 1.1) \text{ MeV}/c^2$. The latter is consistent with zero, as expected.

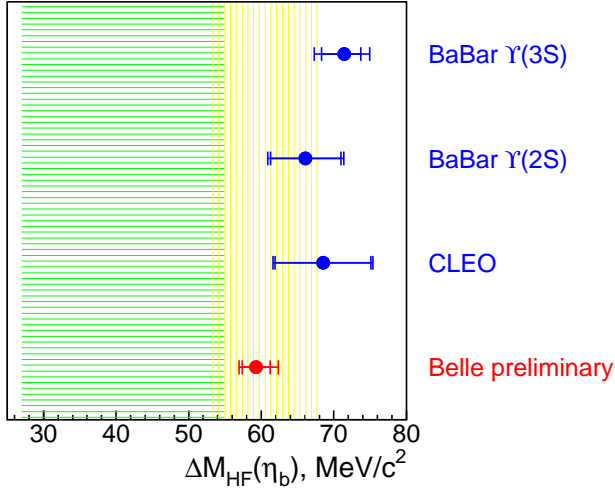


FIG. 7: Hyperfine splitting measured by BaBar in $\Upsilon(3S)$ data [4], BaBar $\Upsilon(2S)$ data [5], CLEO [6] and present preliminary result of Belle. In addition, pQCD [7] (horizontally hatched) and Lattice QCD [8] (vertically hatched) predictions are shown.

* deceased

- [1] I. Adachi *et al.* [Belle Collaboration], arXiv:1103.3419 [hep-ex].
- [2] S. Godfrey and J. L. Rosner, Phys. Rev. D **66**, 014012 (2002).
- [3] N. Brambilla *et al.*, Eur. Phys. J. C **71**, 1534 (2011).
- [4] B. Aubert *et al.* [BaBar Collaboration], Phys. Rev. Lett. **101**, 071801 (2008).
- [5] B. Aubert *et al.* [BaBar Collaboration], Phys. Rev. Lett. **103**, 161801 (2009).
- [6] G. Bonvicini *et al.* [CLEO Collaboration], Phys. Rev. D **81**, 031104 (2010).
- [7] B. A. Kniehl, A. A. Penin, A. Pineda, V. A. Smirnov and M. Steinhauser, Phys. Rev. Lett. **92**, 242001 (2004) [Erratum-*ibid.* **104**, 199901 (2010)].
- [8] S. Meinel, Phys. Rev. D **82**, 114502 (2010).
- [9] A. Abashian *et al.* (Belle Collaboration), Nucl. Instrum. Methods Phys. Res., Sect. A **479**, 117 (2002).
- [10] S. Kurokawa and E. Kikutani, Nucl. Instrum. Methods Phys. Res. Sect., A **499**, 1 (2003), and other papers included in this Volume.
- [11] A. Bondar *et al.* [Belle Collaboration], arXiv:1110.2251 [hep-ex].

- [12] K. Abe *et al.* [Belle Collaboration], Phys. Rev. D **64**, 072001 (2001).
- [13] G.C. Fox and S. Wolfram, Phys. Rev. Lett. **41**, 1581 (1978).
- [14] J. E. Gaiser, Ph. D. thesis, SLAC-R-255 (1982) (unpublished); T. Skwarnicki, Ph.D. thesis, DESY F31-86-02 (1986) (unpublished).
- [15] V. V. Anashin *et al.*, arXiv:1012.1694 [hep-ex].
- [16] R. E. Mitchell *et al.* [CLEO Collaboration], Phys. Rev. Lett. **102**, 011801 (2009) [Erratum-*ibid.* **106**, 159903 (2011)].
- [17] K. Nakamura *et al.* (Particle Data Group), J. Phys. G **37**, 075021 (2010).
- [18] W. Kwong *et al.*, Phys. Rev. D **37**, 3210 (1988); C.S. Kim, T. Lee, and G.L. Wang, Phys. Lett. B **606**, 323 (2005). J.P. Lansberg and T.N. Pham, Phys. Rev. D **75**, 017501 (2007).